AD-A089 736 JAYCOR ALEXANDRIA VA F/G 20/9
ELECTRON AND ION FLOWS IN DIODES.(U)
AUG 80 S A GOLDSTEIN, P F OTTINGER N00014-79-C-0177
UNCLASSIFIED JAYCOR-TPD200-80-008-FR NL

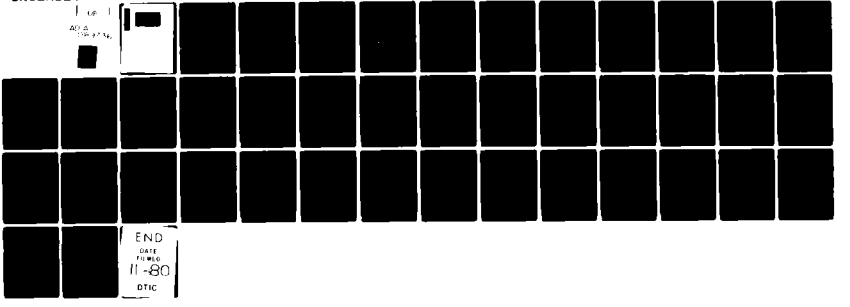

END
DATE FILMED
11-80
DTIC

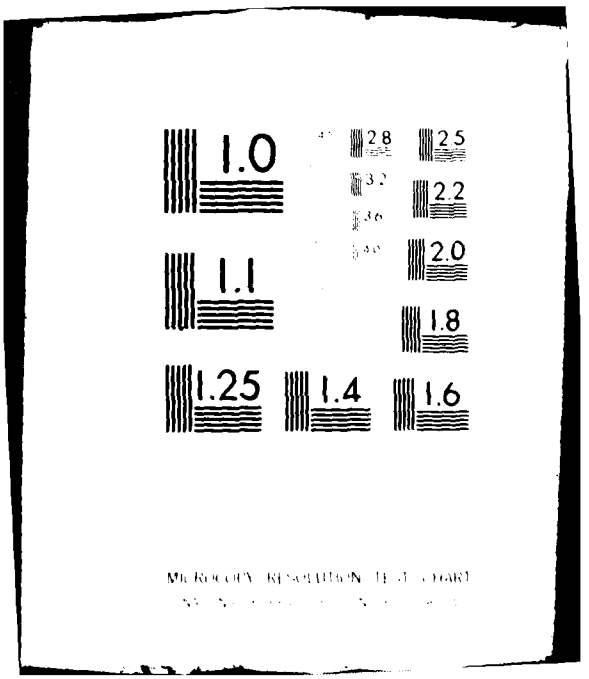
1.0
1.1
1.25
1.4
1.6
2.8
3.2
3.6
4.0
2.5
2.2
2.0
1.8

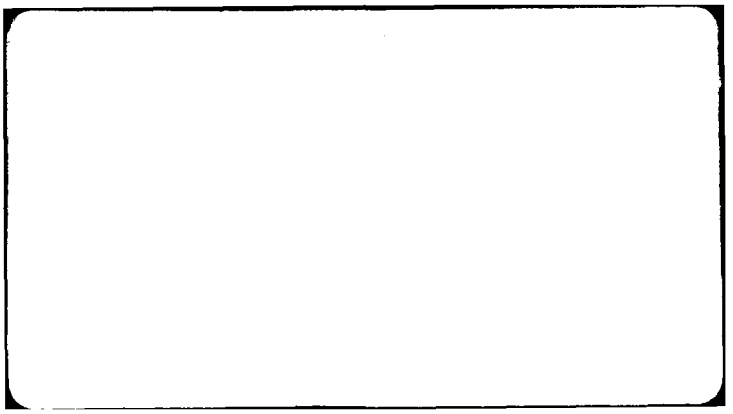

LEVEL II

(2) FINAL REPORT, 19 Mar 79-18 Jun 80.

(6) ELECTRON AND ION FLOWS IN DIODES.

JAYCOR PROJECT 6152

(15) Contract No. N00014-79-C-0177

(14) JAYCOR [redacted]-TPD200-80-008-FR

(10) Dr. Shyke A. Goldstein
Dr. Paul F. Ottinger
Dr. Robert J. Barker
Dr. Robert A. Meger

(11) 19 Aug [redacted]80

(12) 41

Submitted to:

Naval Research Laboratory
Washington, DC 20375

393 455

UNCLASSIFIED

SECURITY CLASSIFICATION OF THIS PAGE (When Data Entered)

REPORT DOCUMENTATION PAGE	READ INSTRUCTIONS BEFORE COMPLETING FORM
1. REPORT NUMBER: TPD200-80-008-FR ✓ 2. GOVT ACCESSION NO.: AD-A089736	3. RECIPIENT'S CATALOG NUMBER:
4. TITLE (and Subtitle): Final Report on Electron and Ion Flows in Diodes	5. TYPE OF REPORT & PERIOD COVERED: Final Report 19 Mar 79 - 18 Jun 80
	6. PERFORMING ORG. REPORT NUMBER: TPD200-80-008-FR
7. AUTHOR(s): Dr. S. A. Goldstein, Dr. P. F. Ottinger, Dr. R. J. Barker, Dr. R. A. Meger	8. CONTRACT OR GRANT NUMBER(s): N00014-79-C-0177
9. PERFORMING ORGANIZATION NAME AND ADDRESS: JAYCOR 205 S. Whiting Street Alexandria, VA 22304	10. PROGRAM ELEMENT, PROJECT, TASK AREA & WORK UNIT NUMBERS:
11. CONTROLLING OFFICE NAME AND ADDRESS: Naval Research Laboratory Washington, DC 20375	12. REPORT DATE: 19 August 1980
	13. NUMBER OF PAGES: 38
14. MONITORING AGENCY NAME & ADDRESS (if different from Controlling Office): Same as block 11	15. SECURITY CLASS. (of this report): UNCLASSIFIED
	15a. DECLASSIFICATION/DOWNGRADING SCHEDULE:

16. DISTRIBUTION STATEMENT (of this Report)

1 copy - Code 4770

DISTRIBUTION STATEMENT A
Approved for public release;
Distribution Unlimited

17. DISTRIBUTION STATEMENT (of the abstract entered in Block 20, if different from Report)

18. SUPPLEMENTARY NOTES

19. KEY WORDS (Continue on reverse side if necessary and identify by block number)

20. ABSTRACT (Continue on reverse side if necessary and identify by block number)

DD FORM 1 JAN 73 1473 EDITION OF 1 NOV 65 IS OBSOLETE
S/N 0102-LF-014-6601

UNCLASSIFIED

SECURITY CLASSIFICATION OF THIS PAGE (When Data Entered)

Contents

I. INTRODUCTION

The intensive work performed on the detailed behavior of diodes has brought about a major change in the national program for achievement of Inertial Confinement Fusion using particle beam drivers. This program has now shifted from electron beams to the light ion beams generated in diodes with high efficiency. These ions will be focused onto medium size targets (about 1 cm in size) from many ion sources in order to achieve the needed high power (about 100 terrawatt) for 10 to 20 ns. The detailed understanding of how such diodes turn on ion sources in order to generate about 10^{17} ions from a single diode is of crucial importance. The time dependence of the ion current, the type of ion species, the magnetic field distribution, anode and cathode plasma motion (affecting ion trajectories and thus focussing) have all been investigated. The effects of different diode materials, geometries, etc. are under continuing study. A combined theoretical and experimental research program of the physics of light ion beams is presently supported by JAYCOR. Many of the results obtained at the Naval Research Laboratory, Sandia National Labs, Physics International and Cornell University have been explained successfully by the diode theory developed by JAYCOR personnel. The physics of electron flow in very large diodes (of the order of 1 meter) as well as of the anode behavior (such as anode plasma formation) is of crucial importance to the question of power transfer to small area loads (such as small diodes or plasma loads).

In diode geometries that converge to small radii, there can be significant electron loss to the anode in the vacuum feed which may turn on an anode plasma there. In addition, the presence of this ion source is another cause for energy drain on the power flow since the ion current is enhanced by a large factor due to electron beam near the anode.

The three subjects, small size diodes (1 mm) in order to generate very large ion current density, medium size diodes (10 cm) for efficient ion beam generation via the Pinch Reflex Diode, and large diodes (~1 m) were the principle areas investigated and are concentrated on in this report. In particular, this report explains the physics of the backscatter diode and how a runaway phenomenon can generate very large current density ion beams which could be used in beam target studies. There follows an examination of the physics of how anode plasmas are generated using various materials and the question of electron flow in a pinch-reflex diode (PRD). The report ends with a review of the role of electron and ion flows in large area diodes driving plasma loads.

II. SUMMARY OF WORK

The work performed on the physics of electron and ion flows in diodes was a combination of an analytical study and complimentary numerical simulation using Particle in Cell codes. These codes, developed during the last few years, have been checked by comparing their predictions to the experimentally observed variables. They were found to be in close agreement. The theoretical analysis was based on general descriptions of relativistic electron drift motions, anode material properties, plasma generation in different gases and Monte-Carlo results for electron scattering in materials.

In the area of the backscatter diode it was discovered that even a single backscatter (per electron) with very high energy loss (more than half of the diode voltage lost during the backscatter process) results in no steady state operation. This explains phenomena observed in a few laboratories studying diodes immersed in very large axial magnetic fields. The backscatter diode is contrasted with the reflex diode and the similarities of their load characteristics for the external generator are pointed out. We also show that very high current densities ($>10^7 A/cm^2$) can be achieved using large ($>10^5 G$) axial magnetic fields.

In the area of the Pinch-Reflex-Diode the time scale for anode plasma generation using different anode materials was investigated. The case of pinch formation without ion flow was investigated using the PIC code. The fraction of electrons in the pinch, diode impedance and energy deposition in the foil were computed. The ion current was then turned on in the pinch area and out to larger radii and was found to scale linearly with r (that is $J_i(r) \sim r^{-1}$). Based on the deposition profile, turn-on times of anode plasma were computed and compared to experimental results. The impedance of the

diode was then computed with ion current flowing, showing a decrease by a factor of 1.5 relative to the same diode operating before ion flow exists.

On the topic of large diodes and imploding plasmas, the role of "mini-diodes" created in the plasma was explained. These psuedo-diodes are responsible for carrying a large fraction of the current across the vacuum gaps in sausage instability regions. The dynamics of implosion is followed from early plasma formation on wire arrays to the driving forces that collapse the plasma. The stability of the run in phase is attributed to the low inductance, return current paths.

The relativistic electrons that flow into the plasma load from the vacuum feed lose a significant fraction of their energy to the plasma electrons due to orbit lengthening caused by the magnetic field there. When currents of a few megamperes flow in the plasma, the resulting self field enhances the stopping power by more than two orders of magnitude over the classical value.

The very large diode ($\sim$ 1 m) that feeds power to the plasma load was studied regarding the problem of magnetic insulation. In particular, an estimate was obtained for the fraction of diode power lost to electron flow in vacuum. The effect that the electron launch geometry at very large radii as well as the impedance of the generator have on that flow was pointed out. The high impedance, high power diodes prove to be the most susceptable to power losses from either electron or ion flows in vacuum. Ion flows are computed for typical $\sim 1\Omega$ impedance diodes. The time scale for generating these flows is then pointed out. If the present simple designs were scaled to higher powers (to say, 30 TW) more than half the power could be lost.

III. THEORY OF FLOWS IN DIODES

In this section, three separate diodes are treated: the backscatter diode, the PRD and the diode feed for plasma loads. These diodes can be conveniently characterized by their sizes which are roughly 1 mm, 10 cm and 1 meter respectively. These sizes are dictated by the applications of these diodes. The backscatter diode may be a tool to generate currents of only 10^5A but from small (10^{-2} cm^2) areas so that very high current density fluxes may be obtained and used in beam target studies at current densities that exceed by an order of magnitude the present 10^6 A/cm^2. The PRD is a diode for generating ion currents very efficiently (60-70%) at high currents of 10^6A and directing these ions to a focus with a small launching angle (half cone of 10^0). The size of such a diode cannot be of the order of 1 cm since then its impedance will be much larger than the desired 1Ω (which would require a gap of 0.5 mm which closes too quickly by plasma motion relative to the needed ~100 ns pulse). It also cannot be excessively large (say 30 cm radius) since then focussing distances of 150 cm are required in assuming a 10^0 launching angle. At such distances a focal spot of 1 cm requires ion beam quality of $1/3^0$. Since present beams have divergences of 1.5^0 - 3^0, the diode diameter has to be about 10 cm. The size of the diode feeding the plasma load is constrained by impedance considerations for the generator and by water breakdown requirements for a given power of a few terrawatts. These constraints lead to one meter sizes.

Discussions of the details for each case follow.

1. Backscatter Diode.

When electrons emitted from a cathode strike a high atomic number anode,a large fraction of the electrons are backscattered into the diode. During the scattering in the material they loose energy and emerge back into the diode with an energy $eV_s < eV_0$ where V_0 is the diode voltage and e the electron charge. In addition, the momentum distribution of the scattered electron fills nearly a hemisphere. In the presence of very large axial magnetic fields the perpendicular momentum is conserved during electron motion in the diode and the parallel momentum serves to drive the electrons back towards the cathode. The point of closest approach is reached when $P_{\parallel} = 0$. Given $P_{\perp}$ and $P_{\parallel}$ at the anode for a backscattered electron it will go back to a point having a voltage V^* (the cathode is at V = 0, the anode at $V = V_0$). The electrons leave the anode with kinetic energy eV_s. This implies

$$\gamma(\text{anode}) = 1 + \left| \frac{eV_s}{m_0c^2} \right|$$

which is related to their momentum by the relativistic relation

$$\gamma^2 = 1 + \frac{P_{\perp}^2 + P_{\parallel}^2}{(m_0c)^2} \quad .$$

As the electrons flow back into the diode from V_0 at the anode, they loose kinetic energy and gain potential energy; for the relativistic case they loose only $P_{\parallel}$ (in fact, $v_{\perp}$ is not conserved but rather increases!), and at any voltage $V^* < V < V_0$ the relativistic factor is

$$\gamma = 1 + \left| \frac{e[V_s - (V_0 - V)]}{m_0c^2} \right|$$

from which one may find $P_{\parallel}$(at V). The value of V^* is given by setting $P_{\parallel}$ (at V^*) = 0 in the momentum equation

$$\left(1 + \frac{p^2}{(m_o c)^2}\right)^{\frac{1}{2}} = 1 + \left|\frac{e(V_s - V_o + V^*)}{m_o c^2}\right|$$

For example, if the electron lost no energy in the scattering process $V_s = V_o$ and if it got scattered with $P_x^2 = P_y^2 = P_z^2$ then $P_{\perp}^2 = 2\,P_{\parallel}^2 = \frac{2}{3}\,P_o^2$ where P_o is the total momentum. The value of P_o is related to V_o by $(1 + |\frac{eV_o}{m_o c^2}|)^2 = 1 + \frac{P_o^2}{(m_o c)^2}$. After some algebra one finds V^*

$$\frac{eV^*}{m_o c^2} = 1 - \left\{1 + \frac{2}{3}\left[(1 + |\frac{eV_o}{m_o c^2}|)^2 - 1\right]\right\}^{\frac{1}{2}}$$

giving about 0.35 MV for V_o = 0.5 MV. The typical electron does not approach the cathode but stays near the anode side (that is its voltage is not less than 0.25 MV). The first problem to realize is that the electron accumulation in the diode before ions are generated causes a reduction in the electric field near the cathode and suppression of emission. The current produced by N backscatters can be computed approximately by using each stream of reflected electrons as having an amount of energy $e(V_o - \Delta V_s)$ after the S-th reflection (see Fig. 1-1). A solution is sought for the current density emitted, J_e, in a diode gap, D, with diode voltage V_o. For simplicity, relativistic effects are disregarded. Poisson's equation in the axial direction - x is:

$$\frac{d^2\phi}{dx^2} = 4\pi\rho = \sum_{s=0}^{N} 4\pi \frac{J_e^s}{v_e^s}$$

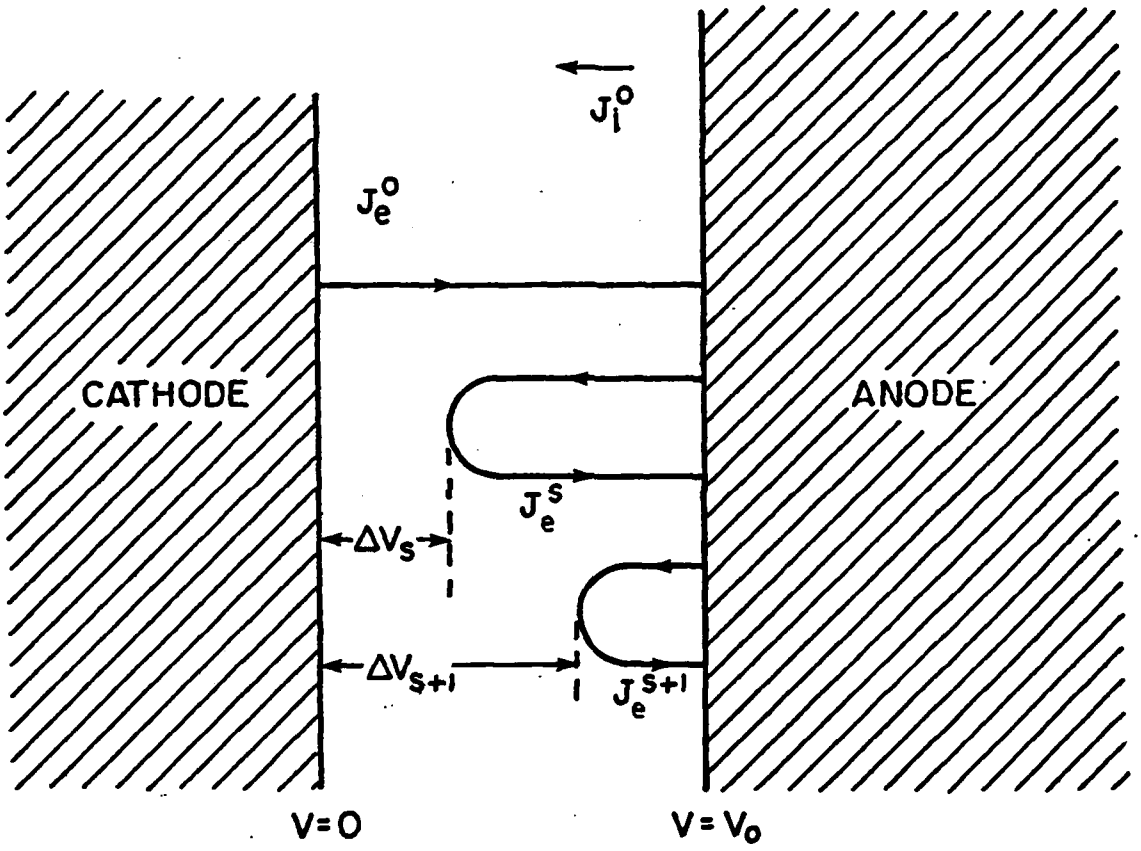

Figure 1-1

where s = 0 is the first stream of electrons from the cathode, s = 1 is the first backscattered flow, etc. The density is double for $s \geq 1$ since that stream returns symmetrically to the anode. Notice that $J_e^{s+1} \leq J_e^s$ since we assume that electrons can only be lost (realistically, secondary electrons are also generated and for special cases an electron flow back after scattering could be enhanced).

The velocity is given by

$$\frac{1}{2} m(v_e^s)^2 = e(\phi - \Delta V_s) .$$

The Poisson equation can now be written in simplified form

$$\frac{d^2\phi}{dx^2} = K^0 J_e^0 \sum_{s=0}^{N} \frac{K^s}{(\phi - \Delta V_s)^{1/2}}$$

which is of the form $\frac{d^2\phi}{dx^2} = F(\phi)$ that can be integrated once by multiplying by $\frac{d\phi}{dx}$ to yield $\frac{1}{2}\frac{d}{dx}\left(\frac{d\phi}{dx}\right)^2 = F(\phi)\frac{d\phi}{dx}$ which gives by integration

$$\frac{1}{2}\left(\frac{d\phi}{dx}\right)^2 - \frac{1}{2}\left(\frac{d\phi}{dx}\right)^2\Big|_{x=0} = \int_0^{\phi} F(\phi)d\phi .$$

For the case of space charge limited emission from the cathode with a cathode temperature much less than the diode voltage (typically $T_{cathode} \leq 10$ eV, while $V_0 \sim 1$ MeV) and with a small work function for the plasma, the electric field in the plasma is a few kv/cm compared to the ~ 1 Mv/cm in the diode. Matching the field at the plasma/electron beam interface on the cathode we may thus set $\frac{d\phi}{dx}\Big|_{x=0} = 0$. The equation for $\frac{d\phi}{dx}$ may now be integrated again

$$\int_0^{\phi} \frac{d\phi}{\left(2\int_0^{\phi} F(\phi)\,d\phi\right)^{1/2}} = \int_0^{x} dx$$

and setting the limits on the anode, $\phi = V_o$ and $x = D$, one finds the single unknown J_e^o. Notice that the integration on the sum of flows starts for the s-th term at $\phi = \Delta V_s$ (since no electrons flow closer to the cathode than ΔV_s) thus no imaginary values are included in our treatment. The result after straightforward but cumbersome integration is that the current density is given by the Child-Langmuir expression with a suppression factor that depends on the values of $\frac{\Delta V_s}{V_o}$ and $\frac{J^{s+1}}{J^s}$. This treatment will not be given here since it adds no special understanding of the physics of the diode. An approximate form was derived for the case where $J^{s+1}/J^s \approx 1$ and $\frac{\Delta V_s}{V_o} = \frac{s}{N}$ which is for $N \gg 1$:

$$J_e = \frac{2.3\ V_o^{3/2}(MV)}{D^2}\ \frac{\ell nN}{N}\ \frac{kA}{cm^2}\ .$$

The current density is thus reduced from the no scattering case and for $N = 10$ it is about 4 times lower. The diode perveance is thus lower if one uses high $\bar{Z}$ material anodes instead of low Z. Initiation of the ion flow from the anode side adds another term in the Poisson equation for the ion space charge and gives us one more boundary condition for the emission law. If anode plasma is assumed then for similar reasons to those on the cathode side the electric field is zero on the anode. There are thus two unknown current densities, J_e and J_i, eminating from the cathode and anode respectively. In addition, electrons are being backscattered from the

anode. Instead of solving the general case with its many unessential details, a single backscatter of all electrons is assumed with a loss of energy ΔV_1. Notice that the ions (assumed singly charged with mass M) move from the anode and thus their velocity is given by

$$\frac{1}{2} M V_i^2 = e\,(V_o - V) \quad .$$

In the region between $\phi = \Delta V_1$ and $\phi = V_o$, the space charge is composed of three flows: the primary electron flow with density $\frac{-J_e}{(2\,e/m)^{1/2}\,\phi^{1/2}}$, the back-scattered flow with density $\frac{-2J_e}{(2e/m)^{1/2}\,(\phi-\Delta V_1)^{1/2}}$, and ion flow with a density $\frac{J_i}{(2\,e/M)^{1/2}\,(V_o-\phi)^{1/2}}$. Poisson's equation may thus be written as

$$\frac{d^2\phi}{dx^2} = \frac{4\pi J_e}{(2e/m)^{1/2}} \left\{ \frac{1}{\phi^{1/2}} + \frac{2}{(\phi - \Delta V_1)^{1/2}} - \frac{(J_i/J_e)\,(M/m)^{1/2}}{(V_o - \phi)^{1/2}} \right\} \quad .$$

Integrating the equation once from x=o by the same technique used earlier and using $\left.\frac{d\phi}{dx}\right|_{x=o} = 0$ one finds:

$$\frac{1}{2}\left(\frac{d\phi}{dx}\right)^2 = \frac{4\pi J_e}{(2\,e/m)^{1/2}} \left\{ 2\,\phi^{1/2} + 4(\phi - \Delta V_1)^{1/2} + 2\left[(V_o - \phi)^{1/2} - V_o^{1/2}\right] \right.$$

$$\left. \cdot (J_i/J_e)\,(M/m)^{1/2} \right\} \quad .$$

The L.H.S. is also zero at x=D where $\phi=V_o$ giving an equation for J_i/J_e:

$$V_o^{1/2} + 2(V_o - \Delta V_1)^{1/2} = V_o^{1/2}\,(J_i/J_e)\,(M/m)^{1/2}$$

or:

$$(M/m)^{1/2}\,J_i/J_e = 1 + 2\,(1 - \frac{\Delta V_1}{V_o})^{1/2}$$

which shows enhancement over the bipolar ratio by a factor equal to the R.H.S.

The above expression may now be inserted into the equation for $(\frac{d\phi}{dx})^2$ and one may proceed to solve by another integration for $\phi(x)$. Then, since $\phi(D) = V_o$, one can find the last unknown: J_e. The surprise is, however, that depending on $\frac{\Delta V_1}{V_o}$ there may or may not be a real solution to $\frac{d\phi}{dx}$ through its equation:

$$\frac{1}{2}\left(\frac{d\phi}{dx}\right)^2 = \frac{4\pi J_e}{(2\ e/m)^{\frac{1}{2}}} \left\{2\ \phi^{\frac{1}{2}} + 4(\phi - \Delta V_1)^{\frac{1}{2}} + 2\left[(V_o - \phi)^{\frac{1}{2}} - V_o^{\frac{1}{2}}\right]\right.$$

$$\left. \times \left[1 + 2\left(1 - \frac{\Delta V_1}{V_o}\right)^{\frac{1}{2}}\right]\right\} .$$

It is interesting to note how the R.H.S. behaves as ϕ goes from 0 to V_o. It starts from 0 and increases until at $\phi = \Delta V_1$ it equals

$$2\left\{(\Delta V_1)^{\frac{1}{2}} + \left[(V_o - \Delta V_1)^{\frac{1}{2}} - V_o^{\frac{1}{2}}\right]\left[1 + 2\left(1 - \frac{\Delta V_1}{V_o}\right)^{\frac{1}{2}}\right]\right\} = 2F .$$

The quantity, 2F, can be expanded for $\frac{\Delta V_1}{V_o} = \varepsilon << 1$ and for $1 - \frac{\Delta V_1}{V_o} = \delta << 1$ to yield

$$F = \begin{cases} V_o^{\frac{1}{2}}\ \varepsilon^{\frac{1}{2}}\ (1 - \frac{3}{2}\ \varepsilon^{\frac{1}{2}}) & \text{for } \varepsilon << 1 \\ V_o^{\frac{1}{2}}\ \delta^{\frac{1}{2}}\ (\frac{3}{2}\ \delta^{\frac{1}{2}} - 1) & \text{for } \delta << 1 \end{cases} .$$

This gives $F > 0$ for ε but $F < 0$ for δ.

It can thus be concluded that very small energy losses (ε case) give steady state solutions but very large losses (δ case) end up with no solution of steady electron and ion flow. One would then like to know where the dividing line is and what would happen physically when the steady state

goes out of existence? The first question is easy to answer: set F = 0 and solve for ΔV_1 to find that $\Delta V_1 = \frac{1}{2} V_o$. Since it has already been shown that typical very high z backscatter gives $\Delta V_1 > \frac{1}{2} V_o$, it can be concluded that no steady-state solutions exist for these materials. The time-dependent solution for general materials is beyond the scope of this work but it should be realized that low z-material backing a thin layer of high z can act as an absorber of electrons and thus bring back a steady state solution. The second question can be treated only heuristically. The ion space charge is enhanced by electrons present near the anode. It flows towards the cathode where it finds only the primary electron flow without backscattered electrons ($\phi < \Delta V_1$). This ion space charge is too large for the existing electron charge present and it thus causes increased emission from the cathode. After the newly emitted electrons arrive and backscatter off the anode they generate a larger ion space charge which in turn after a transmit time to the cathode repeats the process causing the total current to runaway. The current density is limited only by self fields that change the electron flow. Thus very large axial magnetic fields are needed for small area cathodes. The total current is limited by the generator and the diode voltage drops by inductive effects. When the voltage is very low only a few electrons backscatter and the diode can find a steady state (saturation of runaway). The current may stop increasing and this inductive kick will bring the voltage back to the threshold between existence and non-existence of steady state in the electron/ion flow problem. This process is very similar to the reflex diode but no double diode arrangement is needed. The mathematics are very similar and the processes observed are almost the same. They are summarized in Figure 1-2 where the time dependence of current and voltage are shown as a function of time.

1-D REFLEX DIODE THEORY

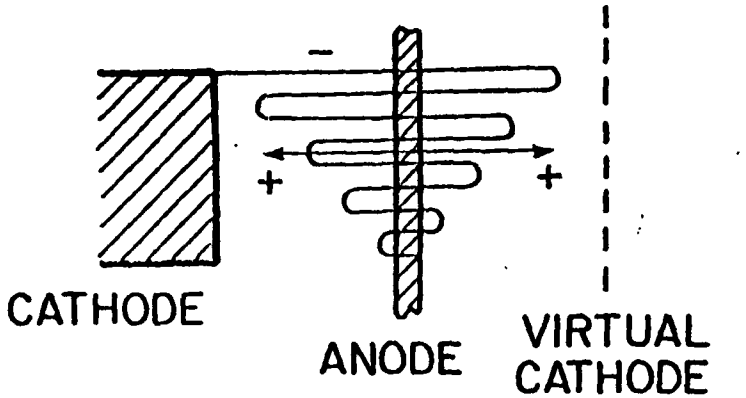

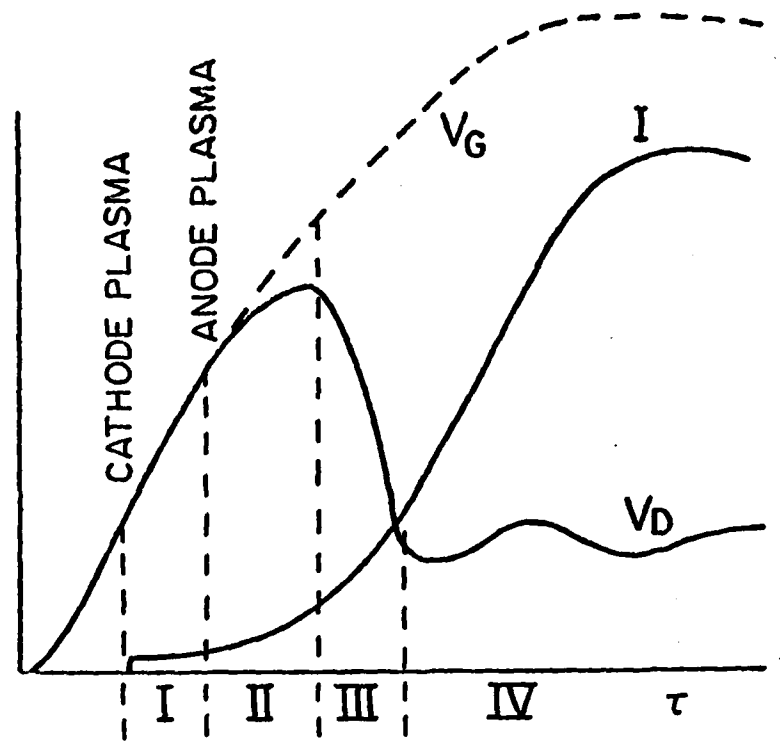

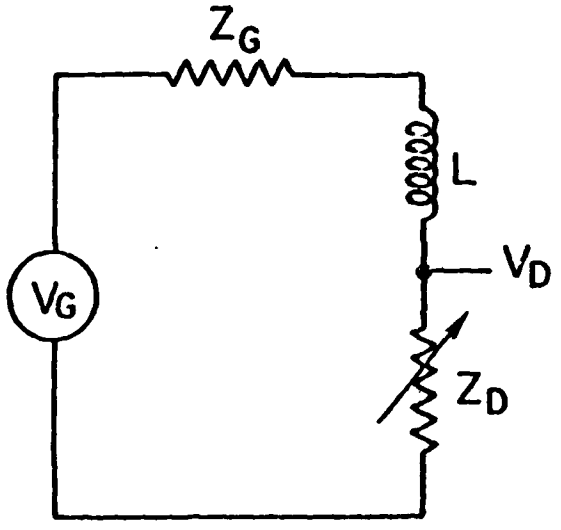

I $J \simeq \frac{J_{c.L.}}{N/\ell n N}$

II $J \propto e^{K\tau}$

III $V_D = V_G - IZ_G - L\dot{I}$

IV V_D DEPENDS ON TOTAL ELECTRON RANGE IN ANODE FOIL (NEED ~FOUR APPEARANCES)

NO AREA OR A-K GAP CONSTRAINT ON TOTAL DIODE CURRENT

Figure 1-2

2. Pinch-Reflex Diode.

a. Anode Plasma Generation. The problem of anode plasma generation using different anode materials is fairly complicated when absorbed gases are included in the process of plasma generation. For clean surfaces of materials such as copper, aluminum and polyethylene, first the simple solid-to-liquid then the liquid-to-gas phase transition and finally the gas ionization into plasma have to be treated. In the first heating phase, relativistic electrons deposit their energy into the anode material via the classical single particle slowing down process. The typical stopping power of about 1.5 MeV/g/cm^2 is enhanced by electron scattering in thick materials. This scattering effect was already treated by Monte-Carlo methods and the enhancement factors are given in the NBS manuscript by L.V. Spencer on Energy Dissipation by Fast Electrons (the results for the 1 MeV typical for ion diodes is used herein). For polyethylene the stopping power is similar to that of carbon which is 1.6 MeV/g/cm^2. This is enhanced by scattering by a factor of 1.28 resulting in 2 MeV/g/cm^2 on the surface of the material. For aluminum, 1.51 MeV/g/cm^2 is enhanced by a factor of 1.87 giving about 2.8 MeV/g/cm^2. For copper 1.29 MeV/g/cm^2 is enhanced by 3.64 giving 4.7 MeV/g/cm^2. All of the above are for a flow of electrons perpendicular to the anode surface with all the backscattered electrons returning to the anode (an assumption justified by the large electric field in the diode where anode heating takes place). The next question is how much charge per unit area is needed in order to bring anyone of the above materials from room temperature to evaporation? Assume that an energy, E (specified in joules/gram), is needed for evaporation. The energy deposited during t(seconds) by a current density J(A/cm^2) impinging on the surface of a material with stopping power S(eV/g/cm^2) is given by the product JtS (joules/gram). In order to reach the value of E for a given material one has to have

$$J\,t = E/S \quad .$$

Therefore, it is the charge delivered per unit area by the 1 MeV electron beam that determines whether or not the material is evaporated. The values for E are given by Hultgren R., Orr R., Anderson, P.D., and Kelly, K. K. in Selected Values of Thermodynamic Properties of Metals and Alloys (New York, John Wiley and Sons, Inc., 1968). The values for aluminum and copper are given as 14 and 6 kJ/g respectively. A separate calculation is needed for polyethylene. After evaporation the molecular bonds must be broken before plasmas of hydrogen and carbon can be generated from the $(CH_2)_n$ polymers. The reaction $CH_2 + e \rightarrow CH_2^+ + 2e$ requires 11.9 eV or 80 kJ/g. Similar values are found for $CH_2 + e \rightarrow CH + H^+ + 2e$. The stripping of electrons from these molecules is very similar to that from water (12.6 eV for $H_2O + e \rightarrow H_2O^+ + 2e$). This information can be found in Herzberg, Infrared and Raman Spectra (page 528). Using the above values we find that J t is equal to 4×10^{-2}, 5×10^{-3}, 1.3×10^{-3} Coulomb/cm^2 for polyethylene, aluminimum and copper respectively. For a time scale of say 10 ns the needed current densities for evaporation are 4×10^6, 5×10^5, 1.3×10^5 A/cm^2 for the above materials. These results explain why it is that conducting anodes coated with $(CH_2)_n$ or $CD_2)_n$ do not generate ion currents until very late into the pulse (about 50 ns assuming 0.8×10^6 A/cm^2). The aluminum takes an order of magnitude less time if it was first baked to remove the absorbed gases (a technique used in experiments at Sandia Labs, Albuquerque and at Physics International). Without prebaking the gas desorption process occurs at a low temperature early in the pulse and the expanding gas is ionized by an avalanche process triggered by the diode electric field. This ionization relies on the 100 eV electrons generated during the avalanche rather than the 1 MeV relativistic electron beam. The cross section for

ionization by a 100 eV electron is three orders of magnitude larger than that by a 1 MeV electron and thus currents of 10^4 A/cm^2 can generate the plasma in nanosecond time scales.

The heating process for a pinch reflex diode is enhanced by the electron reflexing through the foil. The performance of a given diode is initially investigated assuming pure electron flow in the diode. The steady-state electron flow pattern from the cathode to the anode along with the self-consistent fields are modeled by means of a Particle In Cell (PIC) code DIODE2D that has been developed over the past few years. This code was used to simulate the basic Pinch Reflex Diode (PRD) geometry shown in Figure 2-1. The electrons reflex through the anode foil due to the azimuthal magnetic field created by the current flow through the button connecting the thin foil. They are again ejected from the anode-cathode gap by the diode electric field. A typical electron flow pattern is shown in Figure 2-2. The electrons flow to the small central conductor (0.5 cm radius) starting from the hollow cathode (6.4 cm radius) with hollow shank thickness of 0.7 cm projecting axially out from a solid cathode. The cathode separation from the anode foil was 0.32 cm (giving a diode aspect ratio, R/D = 20). The gap between the foil and the solid anode was also 0.32 cm. In addition, the length of the hollow cathode shank projecting from the solid cathode was changed from zero to 0.32 cm and no significant effects on electron flow were observed. Since the electric equipotential lines are compressed near this anode surface it is not surprising that the exact hollow cathode shank length projecting into the A-K gap has little effect on the $\underset{\sim}{E}$ field. In addition, two separate diode voltages were studied, 750 and 1500 kV. For 750 kV the total electron current was 335 kA (2.2 Ω). The total current with ions and electrons was 540 kA (1.4 Ω), a significant drop

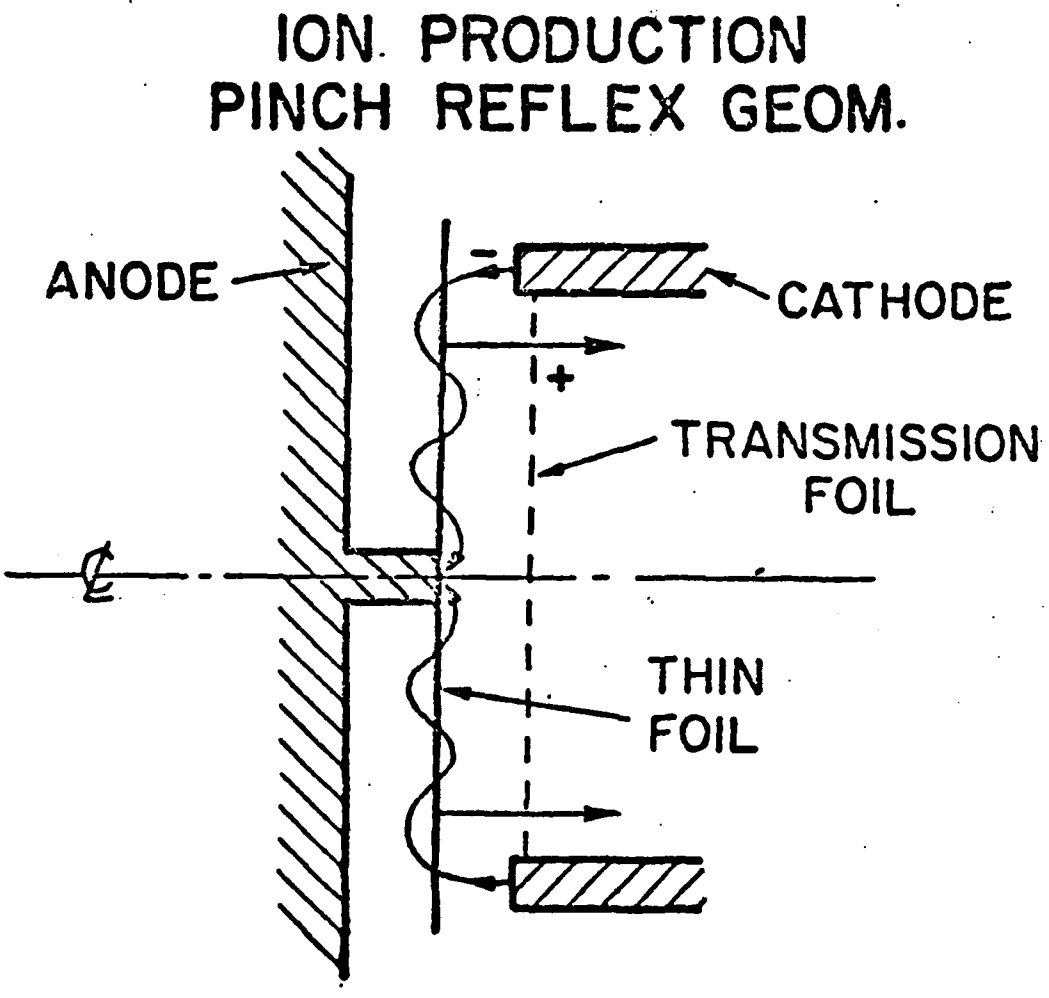
ION PRODUCTION
PINCH REFLEX GEOM.
ANODE
CATHODE
TRANSMISSION
FOIL
THIN
FOIL

Figure 2-1

PINCH-REFLEX DIODE SIMULATION

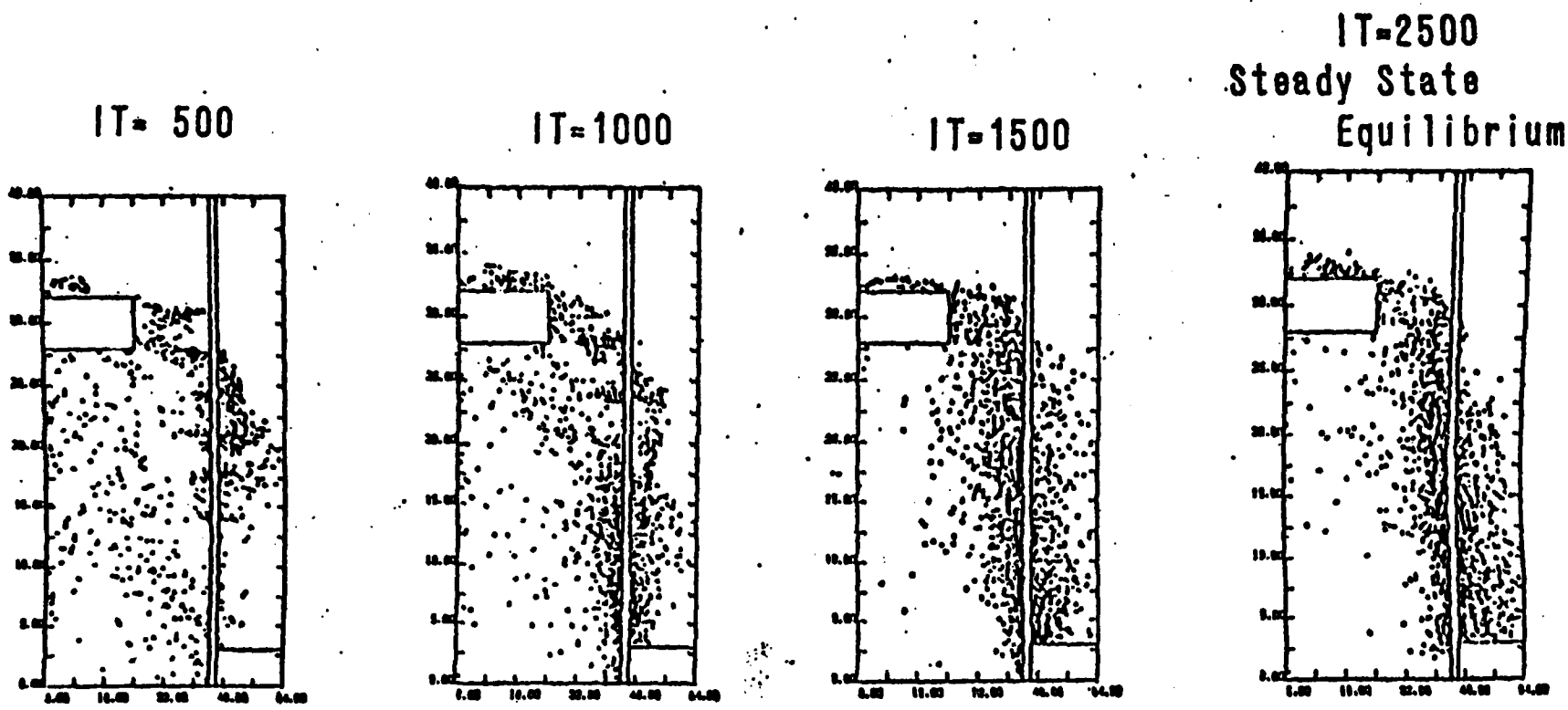

Figure 2-2

Formation of Pinch with Electrons only

RUN $00AN

in impedance. This drop occurs because the currents are self magnetically limited (unlike the one dimensional case where a factor of two drop in impedance would result due to ion space charge). For the 1500 kV, the results show the same impedances. The fraction of electron current that pinched on the central anode conductor was about 40% at these impedances. When the impedance was increased to about 20 Ω (at 7 MV) the fraction in the pinch was nearly 100%. There exists a non-continuous transition between very strong and efficient vacuum pinching and the pinch reflex behavior. It is suspected that electrons are allowed to migrate via $\nabla\vec{B}$ drifts in the low impedance cases while they execute figure eight orbits (the nonadiabatic case) at the high impedance. The Alfven current forms a crude division between these two regimes. The Alfven solution does not include electric fields nor does it solve fields self consistently in the diode. Thus no theory presently exists to characterize this type of diode behavior.

3. Imploding Plasmas and Diodes.

A. General.

The contributions to the physics of imploding plasmas can be summarized in three areas:

(1) Dynamics of implosion.

(2) Relativistic electron beams in the plasma.

(3) Problems in magnetic insulation of radially converging feeds.

In the area of the dynamics of implosion we point out (a) the importance of early time expansion of the wire plasmas, (b) a possible mechanism that acts very early and (c) how to affect it by the polarity of the wire holder geometry. The actual motion of the wires is shown to be dictated at early time by the repulsive forces from the return current rods and at late time by

the attracting forces of the other wires. The stability question of the run-in phase is thus divided into two parts; the repulsive rods play an important role in early time and a specific geometry is suggested for stable run in.

The behavior of relativistic electrons in the imploding plasma is treated in order to find their energy losses inside the plasma compared to energy losses on the anode. The magnetic field forces very tight long orbits to the relativistic electrons forcing more than two orders of magnitude increase of the stopping power of the electrons in the plasma. Typical cases are treated showing that present experimental arrangements allow most of the energy in the electron beam to be absorbed in the plasma. About one Alfven current is allowed to be deposited in the anode in agreement with most experimental data.

The problems associated with magnetic insulation problems in the feed of radially converging structures show very different behavior for negative vs. positive polarity in the inner electrode. Major losses associated with negative polarity are reduced in positive polarity operation. For very high power (30 TW) the example treated shows that new physics, not observed at the 5TW level, will dominate the particle flows in the feed reducing the fraction of current in the plasma by about a factor of 2.

B. Dynamics of Implosion.

The dynamics of wire arrays driven by multiterawatt generators was investigated from a new point of view regarding: 1) prevention of early wire expansion, 2) radial collapse of the wire array and 3) stability of the run in wire array. The three areas are connected to each other since the early wire dynamics dictates the plasma density formed which, in turn, is highly

the attracting forces of the other wires. The stability question of the run-in phase is thus divided into two parts; the repulsive rods play an important role in early time and a specific geometry is suggested for stable run in.

The behavior of relativistic electrons in the imploding plasma is treated in order to find their energy losses inside the plasma compared to energy losses on the anode. The magnetic field forces very tight long orbits to the relativistic electrons forcing more than two orders of magnitude increase of the stopping power of the electrons in the plasma. Typical cases are treated showing that present experimental arrangements allow most of the energy in the electron beam to be absorbed in the plasma. About one Alfven current is allowed to be deposited in the anode in agreement with most experimental data.

The problems associated with magnetic insulation problems in the feed of radially converging structures show very different behavior for negative vs. positive polarity in the inner electrode. Major losses associated with negative polarity are reduced in positive polarity operation. For very high power (30 TW) the example treated shows that new physics, not observed at the 5TW level, will dominate the particle flows in the feed reducing the fraction of current in the plasma by about a factor of 2.

B. Dynamics of Implosion.

The dynamics of wire arrays driven by multiterawatt generators was investigated from a new point of view regarding: 1) prevention of early wire expansion, 2) radial collapse of the wire array and 3) stability of the run in wire array. The three areas are connected to each other since the early wire dynamics dictates the plasma density formed which, in turn, is highly

incompressible when assembled on axis. This density is the prime factor when it comes to consider radiation from the plasma. In this work, no reference is made to quantitative radiation but it is assumed that high plasma densities are desirable for specific outputs. This work will thus concentrate on effects that cause low plasma density, what is their origin and how to avoid them. Included are specific recommendations for experiments to be performed on the large generators.

(1) Early Wire Expansion.

In previous work it was shown that the electric field enhancement on the small radius wires in the presence of MV voltages causes field emission currents to dominate over currents running inside the solid wire. This causes fast wire heating and expansion. Later in time magnetic fields outside the wire plasma grow (during current rise) and start to compress the plasma. Skin current models show wire plasma compression. The model contains a very dominant assumption of current in the skin only. In reality, magnetic field diffuses in because of small wire plasma radii ($\leq$ 0.5 mm) and finite resistivity early in time (when plasma temperatures are $\sim$10 eV). This computation is shown in Appendix A. The main effect of the magnetic field that diffused inside (say at half the peak current) is that when the plasma gets hotter it freezes inside the plasma and during plasma compression it increases rapidly acting as a pressure against compression. This is, in particular, the case as the wire plasmas run radially inward to assemble on axis. During this run-in the total diode inductance increases very fast and the currents through the multiple wires drop (part of this current is then carried outside the wire array) thus reducing the pressure that holds each wire plasma. During this time the plasma wire acts as if spring loaded by the trapped compressed magnetic field and it expands, reducing its density. If

the density would have been high in the first place then most of the described action would have had a lesser effect. We thus recommend a way of reducing early plasma expansion to a minimum. The basic idea is the elimination of the early field emission process. This can be achieved by making the wires be at a positive potential compared to the return current rods. While one possibility to achieve a change of polarity is reversal of generator polarity we do not recommend this because of possible power reduction. The other ways are either using convoluted geometry (Fig. 1) or making a reversed arrangement of geometry inside the cathode (Fig. 2).

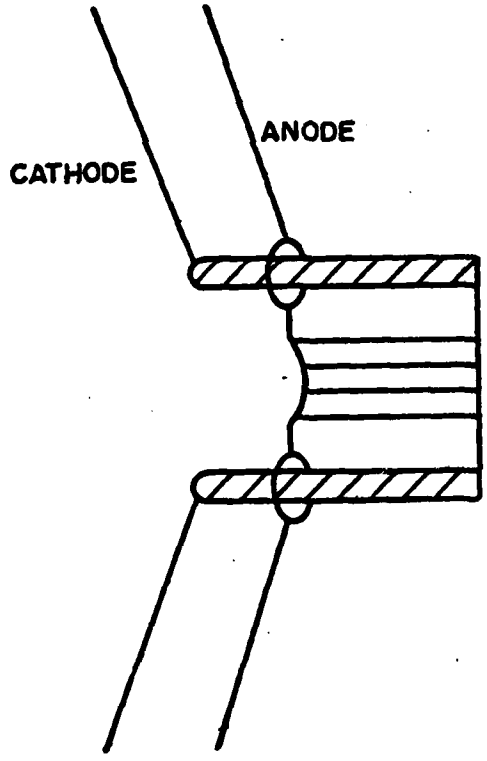

Fig. 1. Convoluted cathode anode.

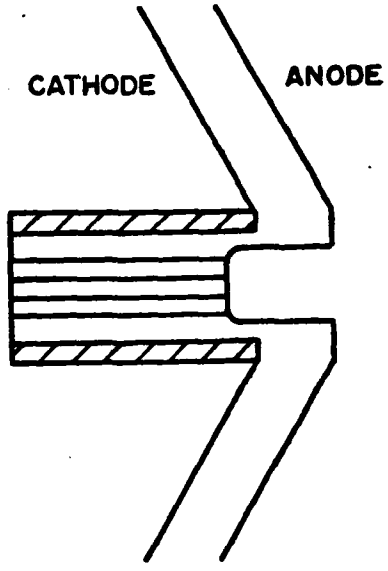

Fig. 2. Wire array inside cathode.

In these experiments the main feature to be tested is the achievement of denser plasmas. The physics included in the next section should also be

considered before performing the suggested reversed polarity experiments and it is desirable to check them first.

(2) Radial Collapse of Wire Arrays.

The present way of thinking about the radial motion of the wires onto the diode axis assumes that the attraction between the wires pulls them inwards. One then arrives at a very simple conclusion that since current increases linearly, $I \sim t$, and attraction force increases as $\sim I^2$, the initial motion is given by the acceleration equation

$$\frac{d^2r}{dt^2} = k\, t^2$$

so that

$$r \sim r_o \left(1 - \left(\frac{t}{t_o}\right)^4\right) \quad .$$

This result will change drastically if we look a little bit closer at the experimental arrangement along the wire array (Fig. 3) taking as an example 6 wires.

In the typical experiment the distance between wires d_2 is much larger than d_1 ($d_2/d_1 \sim 5$ to 10). The current outside does not return uniformally through a cylinder generating no B fields inside. It goes through the rods and because of skin effects runs at the surface of these rods. The single rod near a wire generates a magnetic field larger than all the other wires. Since the currents in wire-rods are antiparallel, they repel each other and the wire is pinched inside. All the old calculations have missed this point and new calculations should be performed to see how much of an effect on assembly time will be predicted. In summary: one

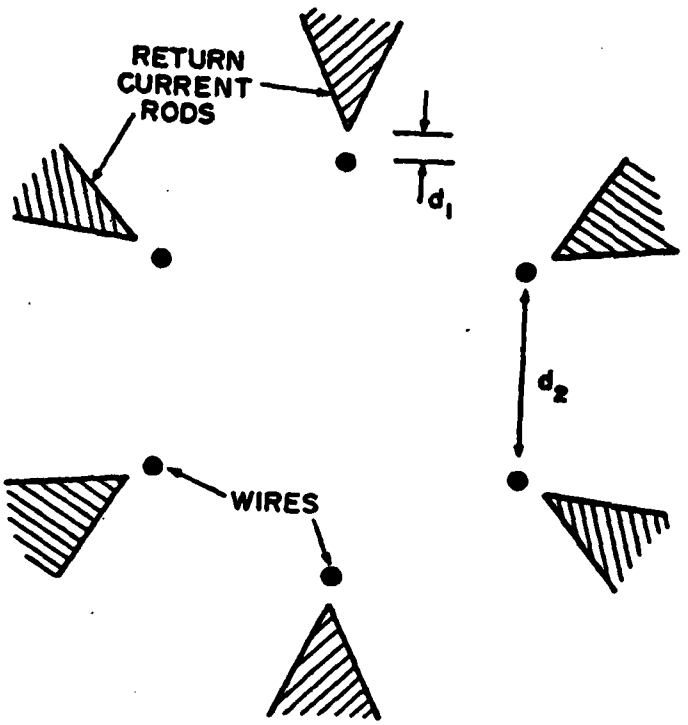

Fig. 3. Wires and Return Current Rods

should say that at early times ($d_2/d_1 \gg 1$) the wires are pushed by the rods inside but later in time ($d_2/d_1 \sim 1$) they pull each other.

(3) Stability of the Run in Wire Array.

We now look at the question of how stable the wire array is for assembly on axis. This work is very different from the one already performed by Rostoker in a number of aspects. N. Rostoker considered only the attractive forces between the wires and neglected the rods and as a result was completely insensitive to an azymuthal transformation of the whole wire array. In this treatment one considers the main effect to be that of the rods and thus shows that any tiny transformation is inherently unstable because of the present shape of the rods. Actually, it is difficult to conceive of a geometry that would be more unstable. Consider the geometry of

Fig. 3 and notice that the current in the rods runs very near to its tip. If wires are not perfectly aligned with each other, than the pushing force from the rods will not push them into the center and they will only partially collide there, overlapping their plasmas. If they are all aligned very well with each other, than the pushing force from the rods will not push them into the center and they will only partially collide there, overlapping their plasmas. If they are all aligned very well with each other then a tiny twist of the wire array relative to the rods will result in a rotational momentum causing the wires to miss each other near axis.

This may explain the large scatter in the data of radiation for given electrical pulses on the generator that have basically the same pulse shape and power. Viewing the wire array x-rays from the anode direction as a function of time (a few frames) near assembly may show if indeed such imperfect radial motion exists in an experiment where a relative twist was intentionally superimposed. It is also recommended to check time integrated data of shots already taken and see if low radiation output was accompanied by non radial implosion.

The question of how to stabilize such an implosion is treated next. Out of the many possibilities it was found that the cup arrangement (Fig. 4) was the simplest and easiest experimentally. The two sharp sides act as stabilizers as they push the wire radially inwards.

C. Relativistic Electron Beams in the Plasma.

When the flow of relativistic electrons enters the imploding plasma it participates in the structure of the total current and the energy flow balance as well as in the pressure balance. The origin of these electrons could be in the larger radius feed and would be magnetically insulated and

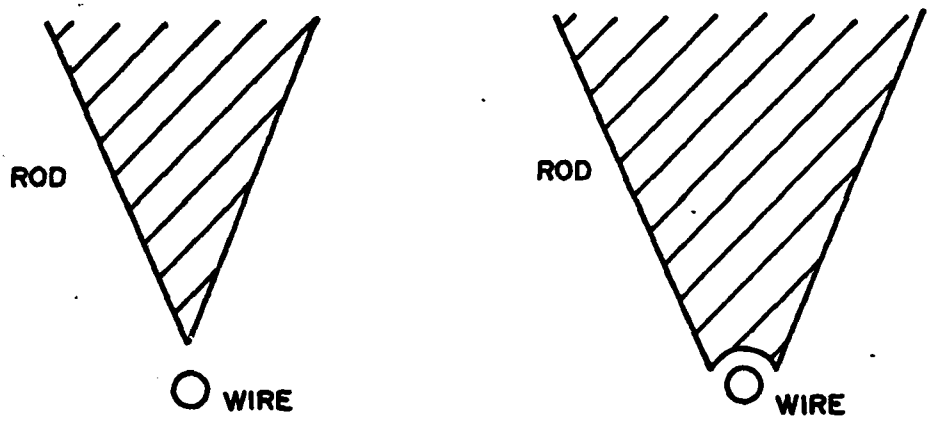

"OLD" rod and wire "NEW" rod and wire

Fig. 4. Old and New Return Current Rods

driven into the plasma by an $E_r \times B_o$ drift. When they enter the plasma these radial fields drop by a very large factor due to the high conductivity of the plasma and its large radial extent ($\sim$1 cm). Outside of the plasma fields of the order of 1 MV/cm exist but inside it they drop significantly. An upper limit to the axial drift of such electrons due to the E_r field may thus be estimated by assuming $E_r \approx 3\times10^5$ V/cm and find that:

$$\langle v_z \rangle \leq c \frac{E_r \times B_o}{B_o^2} = c \frac{E_r}{B_o} \qquad (1)$$

which is about $5\times10^{-4}c$ for currents of 3 MA at 3 mm radii.

Another drift that takes place is that of ∇B type. Very near the axis where the electron flow encloses to less than the Alfven current (50 kA for 1 MeV) electrons propagate by sinusoidal orbits with fast average speeds ($v \sim \frac{1}{10} c$) and thus make it to the anode losing almost no energy. The fraction of energy observed using stacked films for hard x-ray observation as reported by the Maxwell Laboratory group (private communication with Wayne Clark) agrees well with one Alfven current of relativistic electrons

arriving at the anode. As one follows electron orbits at larger radii the electrons drift via gradients in the magnetic field structure. The drift is towards the cathode for increasing B_0 fields and towards the anode as the field decreases. The value of the drift velocity in (see Figure 5).

$$\langle V_Z \rangle = \frac{\frac{1}{2} m v_\perp^2 \Delta B}{eB^2} \tag{2}$$

where m is the relativistic mass of the electron and $V_\perp$ is its perpendicular velocity. In addition, curvature $\underset{\sim}{B}$ drifts also are directed towards the anode and have a value comparable to that of Eq. (1) due to azymuthal velocities of the relativistic electrons thus one should use twice the value of Eq. (1). The magnetic field falls off slower than 1/r on its shoulder and thus an overestimate at $\langle V_z \rangle$ will be given using an 1/r dependence. It is then easy to obtain.

$$\langle V_z \rangle < \frac{1.7 \times 10^4 \gamma\beta^2 c}{2I \text{ (Amperes)}} = c \frac{\beta I_{Alfven}}{2I} \tag{3}$$

The electrons thus drift very slowly with tight orbits and the deposition of their energy a-ong the axial direction is enhanced by the ratio of $\frac{c}{\langle V_Z \rangle} \equiv R$ which is larger than $\frac{2I}{\beta I_{Alfven}}$. For 1 MeV electron ($\beta \equiv 0.95$, I_{Alfven} 5×10^4A) and for I = 3 MA then gives 2×10^2 enhancement of the stopping power of the electrons in the plasma (typically 2 MeV/g/cm^2). While the diluted density $\rho \sim 10^{-3}$ g/cm^3 of the imploding plasma would have subtracted over a distance of 3 cm about 6 keV from the relativistic electron, when the enhancement factor is included all the 1 MeV energy is lost in the plasma. We thus conclude that imploding plasmas with large currents form very good traps for the relativistic electrons as long as the impedance of the generator is less

than a critical value so that the energy loss in the 10^{-3} g/cm^3 plasma over ℓ = 3 cm length exceeds the voltage of the electrons (nearly that of the diode)

$$\rho \ell R S > V ,$$

or for the case considered

$$0.7 I > V \beta^2 \gamma . \qquad (4)$$

Approximating $\gamma \simeq 1 + 2V$ by $2V$ where V is in MV, one obtains

$$0.35 I(MA) > V^2(MV) .$$

The statement is that if the voltage of the feed is about 1 MV then one needs about 3 MA. If, however, 3 MV are used then about 30 MA are needed. Otherwise, the beam can make it all the way through. That is probably the reason why AMP, that performed as a high voltage, low current generator showed a lot of bremsstrahlung x-rays on the anode, causing only a fraction of the current to be carried by the slow plasma electrons. Low impedance generators thus have inherent advantages of being able to absorb the kinetic energy of the beam back into the plasma. One word of caution regarding the use of the above numbers. The stopping power of the relativistic electrons is for non-ionized medium that gives the 2 MeV/g/cm^2. When the plasma is very hot the classical stopping power changes and increases by factors of 2 or 3 (depending on ionization state, temperature, density, etc.). This is only a theoretical prediction since no one has yet measured that increase. In addition, one must consider the magnetic effect. The numbers in Eq. (4) may thus be alleviated and it may look like $I > V^2$.

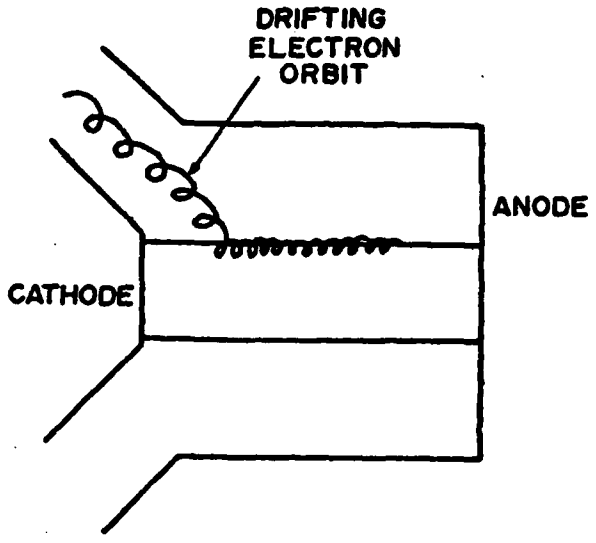

Fig. 5. Magnetically insulated REB trapped in the plasma

D. Impact on Generator Design.

Since the voltage on the upper part of the diode in vacuum is given by the expression $V = \frac{d}{dt}(L \cdot I)$ where L is the diode inductance in vacuum and since this inductance does not change much in the beginning we find that $V = L \frac{dI}{dt}$. The generator dictates that voltage by its open circuit pulse $V_{o.c.}$ and its impedance Z_G. Thus the voltage is $V = V_{o.c.}(t) - I Z_G - L_{insulator} \frac{dI}{dt}$. For given $V_{o.c.}(t)$, V(t) and I(t) can be solved exactly. Our new concern now is that the resultant current and voltage satisfy the inequality of Eq. (4) of Section C, which is putting a constraint on either L or $V_{o.c.}(t)$. Specifically one should lower L to a minimum (this will be discussed in the next section on magnetic insulation) but more important, one needs to give $V_{o.c.}(t)$ a slow increase in time. While the exact treatment is rather lengthy the major results can be obtained by simply assuming $V = L \frac{I}{\tau}$ where τ is the rise time and now use Eq. (4) of Section C to obtain $0.3 I > (\frac{LI}{\tau})^2$ or $\tau > 1.7 L \cdot I^{\frac{1}{2}}$ which states that for larger currents one likes to have longer rise times, more than 100 ns for 20 nH and 10 MA. This agrees

with the previously unexplained experimental observation that better results were obtained with long pulses including the so called high power prepulse of BJ 5. In conclusion, the generator equations above need to be solved for given $V_{o.c.}(t)$ and the resultant V(t), I(t) checked to see if inequality in Eq. (4) of Section C is satisfied, otherwise $V_{o.c.}(t)$ must be changed.

E. Problems in Magnetic Insulation.

The magnetic insulation of the vacuum feed is important since it prevents electron flow from crossing the A-K gap at large radii. Unlike low voltage (< 1 MeV) generators which do not turn on the cathode, the high power generators operate with all cathode surfaces turned into a plasma. Two major effects should be looked at: the electron current loss to the anode and the ion current loss to the cathode. Specifically, the electron loss is important since it heats the anode surface outside the plasma load. This heating will cause gas desorption off the anode material igniting an anode plasma. The time scales for such a phenomenon are derived. The ion current is far in excess of the simple Child-Langmuir value due to the presence of the electron radial flow similar to that in a pinched beam diode. For beam electron flow of 2Ω the ion current is nearly twice the electron current causing the total current loss to be about 1Ω. Thus, if a feed operates at 3 MV and has a total current of 10 MA with 1.5 MA of that current (only 15%) in the electron beam, this current will cause (if allowed to ignite an anode plasma) an ion current of 3 MA leaving only 5.5 MA in the plasma load on axis.

It is therefore obvious that the electron current in the beam should be minimized and the ignition of anode plasma should be prevented at large radii by choosing correct geometries and anode materials that can withstand heating for longer times. First we show the basic mathematical treatment of

the magnetic insulation in a radial feed, than we compute anode heating and point out material response for anode plasma ignition times.

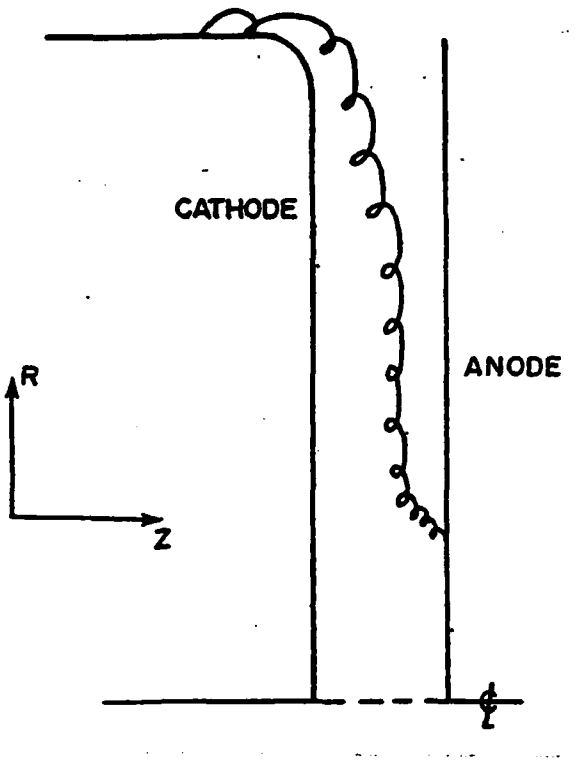

Electron orbits in radial feeds

We assume that a constant voltage exists between anode and cathode during the time when the plasma runs inwards and the effective inductance change is such that

$$Z_G = \frac{dL}{dt}$$

which is satisfied by most low impedance high power generators.

Fig. 6. Typical electron orbit in vacuum feed

The geometry considered and a typical electron orbit are shown in Fig. 6. The electron drifts radially inwards by the $\vec{E}x\vec{B}$ drift and it drifts axially across by the $\vec{\nabla B}$ drift. These two drifts dictate a given path for the guiding center motion provided the axial (the A-K gap) and radial (radius R) lengths are much larger than the Larmour radius $r_L = \frac{1.7(\gamma^2-1)^{\frac{1}{2}}}{B(kG)}$. Since the typical A-K gaps are one centimeter and since currents larger than 3 MA will be considered, the typical magnetic fields at radii on the order of 10 cm are larger than 60 kG. The gyroradii are of the order of millimeters, much smaller than A-K gaps. The equations for the axial and radial velocities

are:

$$\frac{V_Z}{c} = \frac{V_{\nabla B}}{c} = - \frac{\frac{1}{2} m v_\perp^2 \nabla B}{e c B^2} = - (\gamma - \frac{1}{\gamma}) \cdot \frac{\partial B/\partial Z}{B^2} \times 850 = \frac{\gamma \beta^2}{4} \frac{17 \times 10^{-3}}{I\ (MA)} , \quad (1)$$

$$\frac{V_r}{c} = \frac{E_Z \times B}{B^2} = \frac{- \frac{V_o}{D} \frac{1}{300}}{\frac{I}{5r}} = - \frac{r}{D} \cdot \frac{V_o}{I} \quad \frac{1}{60} . \quad (2)$$

Here we have assumed that the E field is a constant in the gap, $E = \frac{V_o}{D}$, and $B \sim r^{-1}$. Also γ is the relativistic mass ratio for the electron which is a function of its position and V_o and I are the voltage and current in MV and MA. Note that the radial velocity is inversely proportional to the impedance. The equation of the orbits is derived through

$$\frac{dr}{dZ} = \frac{\frac{V_r}{c}}{\frac{V_Z}{c}} , \quad (3)$$

and the result is

$$\frac{dr}{dZ} = \frac{- r}{\gamma - \frac{1}{\gamma}} \frac{4V_o}{D} .$$

Since $\gamma \sim 1 + 2\ V_{MV} \sim 1 + 2V_o \frac{Z}{D}$, we may separate the equation

$$- \frac{dr}{r} = \frac{dZ}{(\gamma - \frac{1}{\gamma})} \frac{4V_o}{D} , \quad (4)$$

and integrate

$$- \ln r \Big]_{r_1}^{r} = \ln\ 4\ V_o\ \frac{Z}{D} + \ln (1 + V_o \frac{Z}{D}) \Big]_{Z_1}^{Z}$$

Here, the particle started at a distance Z_1 from the cathode at a radius r_1 and will reach a distance Z at a radius r given by

$$\frac{r_1}{r} = \frac{Z}{Z_1}\left(1 + \frac{V_o}{D} Z\right)\left(1 + \frac{V_o}{D} Z_1\right) . \qquad (5)$$

The question of finding the radius where the particle crosses the gap D can now be answered:

$$r = r_1 \frac{Z_1}{D} \frac{\left(1 + \frac{V_o}{D} Z_1\right)}{1 + V_o} \qquad (6)$$

The result shows that large gaps D are very beneficial and also shows how sensitive the result is on the value of Z_1 and r_1 namely the specific flow pattern that lift electrons off the cathode shank dictates how well they can be magnetically insulated flowing radially inwards. There is a definite advantage of positive polarity operation since it eliminates shank structure and thus minimizes Z_1. For simplicity we assume that electrons lift off by the electric field so that near the cathode all the velocity gained turns parallel to it at a distance 2 Z_1 (see Fig. 7).

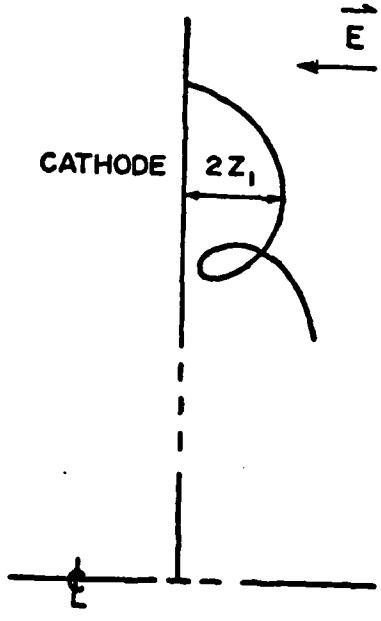

Figure 7

Near $\gamma \simeq 1$, one may write the following expressions

$$\text{(for relativity)} \quad \gamma^2 = 1 + \frac{p_r^2 + p_z^2}{(m_o c)^2} \simeq 1 + \beta_r^2 + \beta_z^2 \tag{7}$$

$$\text{or } \gamma^2 \sim 1 + \beta_r^2 \text{ at } 2\, Z_1$$

$$\text{(for energy)} \quad \gamma = 1 + 2\, V_{MV}(Z_1) \simeq 1 + 4\, Z_1 \frac{V_o}{D} \tag{8}$$

$$\text{(for the radial momentum due to B)} \quad \beta_r \simeq \frac{eB\ 2Z_1}{mc^2} \tag{9}$$

After some algebra and using $B \sim \frac{.2\ I(MA)}{r_1}$, these reduce to

$$\frac{Z_1}{r_1} = \frac{V_o r_1}{D} \ \frac{1.5 \times 10^{-4}}{I^2(MA)} \ . \tag{10}$$

Inserting (10) into (6) one finds

$$r = \frac{r_1^3}{D^2} \ \frac{V_o}{1 + V_o} \ \frac{1.5 \times 10^{-4}}{I^2\ (MA)} \left(1 + \frac{V_o^2}{D^2} \ r_1^2 \ \frac{1.5 \times 10^{-4}}{I^2(MA)}\right) \tag{11}$$

The dependence on V_o is weak, the very large currents help but large radii are the biggest problem. One must design around it to try to minimize it. For the typical values I = 3 MA, r_1 = 100 cm, and D = 2 cm, one obtains r = 4 cm (which can be made 1 cm if D = 4 cm). For I = 10 MA and all of the above the same, r = 0.4 cm which brings us back to trapping the electrons in the imploding plasma. Changing radii to r_1 = 200 cm causes a problem again since r = 4 cm.

F. Igniting the Anode Plasma.

Assuming now that a finite fraction, I_b, of the total current flows as a beam igniting an area up to radii of $\sim$5 cm, we find that an area A of about 75 cm^2 is heated. If one uses a given anode material the heating will ignite a plasma (independent of electron voltage) on a time scale, τ, given by using the concept of areal velocity V_A developed for the study of pinched beam diodes,

$$V_A \frac{I_b}{A} \tau = 1 \quad . \tag{12}$$

In order to increase τ (so no ion current flows during it) one has to use materials with small V_A such as carbon or coatings of teflon or polyethelyne that all have high specific heat, causing longer times for needed heating. If, however, one uses stainless steel, its low specific heat increases V_A by $V_A = 10 \frac{cm^2}{100\ kA\ ns}$ which for I_b = 300 kA, A = 75 cm^2 gives τ = 2.5 ns while for carbon it will be about 50 ns. If ion beams are allowed they are $I_i \simeq 2I_e$ for $\sim 1\Omega$ structures and thus about 1 MA will be lost in the above example.

The above examples obviously point out the importance of structure and anode materials and their effects on the existance of mechanisms for current flow in the diode.